PROCEEDINGS OF SCIENCE

The Anderson transition in QCD with $N_f = 2+1+1$ twisted mass quarks: overlap analysis

Lukas Holicki[*] [†]
Institut für Theoretische Physik, Justus-Liebig-Universität Gießen, 35392 Gießen, Germany
Lukas.Holicki@physik.uni-giessen.de

Ernst-Michael Ilgenfritz [‡]
Bogolubov Laboratory for Theoretical Physics, Joint Institute for Nuclear Research, 141980 Dubna, Russia
ilgenfri@theor.jinr.ru

Lorenz von Smekal
Institut für Theoretische Physik, Justus-Liebig-Universität Gießen, 35392 Gießen, Germany
Lorenz.Smekal@theo.physik.uni-giessen.de

Chiral Random Matrix Theory has proven to describe the spectral properties of low temperature QCD very well. However, at temperatures above the chiral symmetry restoring transition it can not provide a global description. The level-spacing distribution in the lower part of the spectrum of the Dirac operator is Poisson-like. There the eigenmodes are localized in space-time and separated from the rest of the spectrum by a so-called mobility edge. In analogy to Anderson localization in condensed-matter systems with random disorder this has been called the QCD-Anderson transition. Here, we study the localization features of the low-lying eigenmodes of the massless overlap operator on configurations generated with $N_f = 2+1+1$ twisted mass Wilson sea quarks and present results concerning the temperature dependence of the mobility edge and the mechanism of the quark-mode localization. We have used various methods to fix the spectral position of the delocalization transition and verify that the mobility edge extrapolates to zero at a temperature within the chiral transition region.

The 36th Annual International Symposium on Lattice Field Theory - LATTICE2018
22-28 July, 2018
Michigan State University, East Lansing, Michigan, USA.

[*] Speaker.

[†] This work was supported by the Helmholtz International Center (HIC) for FAIR within the LOEWE initiative of the State of Hesse.

[‡] Hospitality and support during a research visit at JLU within the HIC for FAIR visitor program are greatly acknowledged.

PoS(LATTICE2018)180

1. Introduction

Since P. W. Anderson described the vanishing zero-temperature conductivity in imperfect crystals occurring when the quenched disorder exceeds some threshold [1], transitions from extended to localized states have attracted much interest. Examples have been found in a variety of systems. In lattice gauge theory this has been extensively studied, beginning with SU(2) gauge theory [2, 3, 4, 5], as well as in QCD, both quenched and unquenched. The spectrum of the Dirac operator in the high-temperature phase consists of two coexisting regimes. It turned out that the issue of localization is closely connected to a purely spectral feature like the loss of eigenvalue repulsion.

Below T_c the Dirac operator spectrum is entirely described by Random Matrix Theory (RMT) [6, 7], where the global symmetries of a theory are translated into universal spectral features and observables become averages over random matrices. These averages must be stripped of microscopic fluctuations, for example the level spacing distribution must be unfolded. Three-color QCD corresponds to the chiral Gaussian Unitary ensemble (GUE) with a Dyson index $\beta_D = 2$ [8].

Above T_c, a lower end of the spectrum appears that can not be described with random matrices anymore. The eigenvalue spacing in this lower part is uncorrelated, and the corresponding eigenmodes are localized. The energy scale λ_c, that separates this region from the delocalized region is called "mobility edge", in analogy to the Anderson transition in condensed matter physics.

In quenched QCD the localized regime appears first at the deconfinement phase transition, whereas in full QCD it appears above the chiral phase transition. In both cases, a so-called Banks-Casher gap opens in the spectral density $\rho(\lambda)$, as schematically illustrated in Fig. 1.

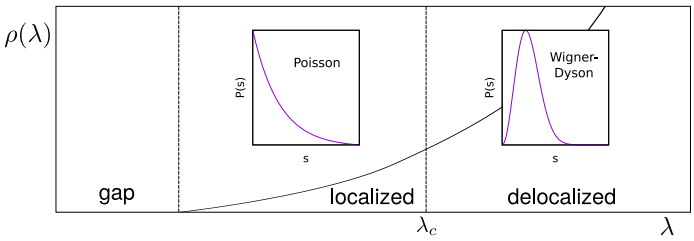

Figure 1: The localized and delocalized spectral regimes of the QCD Dirac operator for $T > T_c$ and the corresponding level spacing distributions $P(s)$, as predicted by Random Matrix Theory.

In quenched QCD at high temperatures the spectral density of eigenstates (of the staggered Dirac operator) shows a square root behaviour [9], and the delocalization energy scale has been empirically identified using the inverse participation ratio (IPR) [10]. A clear correlation between the space-time density of the localized eigenmodes and the local Polyakov loop has been observed [11]. The modes close to the mobility edge possess a multifractal structure [12, 13]. This has been shown for both full QCD as well as in models with orthogonal and symplectic universality classes [14]. The critical exponent of this transition occurring in the Dirac operator spectrum has been found to agree with the critical exponent of the corresponding Anderson model [15, 16]. Fluctuations of the Polyakov loop and regions of exceptional self-duality have been identified to act as source for mode localization in the case of Möbius Domain-Wall fermions [17].

On the background of SU(3) gauge field configurations, generated in full QCD with 2+1+1 dynamical fermions, we have studied the spectrum and eigenmodes of the massless overlap operator,

[18]

$$D = \frac{\hat{\rho}}{a}\left(1 + \mathrm{sgn}K\right), \tag{1.1}$$

that exactly fulfills the Ginsparg-Wilson equation $\{\gamma_5, D\} = \frac{a}{\hat{\rho}} D\gamma_5 D$, where $\hat{\rho} \in (0,2]$ is an arbitrary scaling factor. The sign kernel $\mathrm{sgn}K = \frac{K}{\sqrt{K^\dagger K}}$ was computed with a rational approximation while for the kernel K we used the Wilson operator with a negative mass. In the continuum, the Dirac eigenvalues are purely imaginary, but on the lattice the eigenvalues are distributed on the Ginsparg-Wilson circle $2\mathrm{Re}\,\lambda = \frac{a}{\hat{\rho}}|\lambda|^2$. The continuum limit $a \to 0$ is mimicked by stereographically projecting the eigenvalues onto the imaginary axis.

In order to set the scene for disorder and finite temperature, we have used gauge field configurations generated by the tmfT collaboration (twisted mass at finite temperature) [19, 20, 21] with $N_f = 2+1+1$ flavors of dynamical Wilson fermions and using the Iwasaki gauge action. While strange and charm quark have physical masses, the pion mass is still unphysically large, $m_\pi \approx 370$ MeV, in the ensembles considered here.

Our spectral computations were performed on two groups of ensembles with different lattice spacings, for several temperatures selected by N_t, see Table 1. The eigenmodes of the overlap operator on these gauge configurations were computed using the Implicitly Restarted Arnoldi method (IRAM).

A370: $N_s = 24$, $a = 0.0936$ fm			
N_t	T / MeV	number of conf.	$\frac{\text{modes}}{\text{conf}}$
4	527.06	98	512
5	421.65	63	512
6	351.37	111	512
7	301.18	50	512
8	263.53	100	512
9	234.25	101	512
10	210.82	99	512

D370: $N_s = 32$, $a = 0.0646$ fm			
N_t	T / MeV	number of conf.	$\frac{\text{modes}}{\text{conf}}$
3	1018.21	96	300
6	509.11	71	300
14	218.19	121	190

Table 1: The tmfT lattice ensembles used in this work.

2. The moblity edge λ_c

Below the temperature of the chiral crossover, the Dirac spectrum of QCD is entirely dominated by its global symmetries and can be classified with a Dyson universality class. In this regime universal features of QCD are well described by Gaussian ensembles of random matrices. Above T_c, however, RMT fails to describe the lowest part of the spectrum, that eventually contains localized eigenmodes and where the level spacings are uncorrelated to each other. Recent studies in quenched QCD imply, that the localized part of the spectrum completely disappears, when the deconfinement transition temperature is approached from above [22].

To get an appropiate estimate for the mobility edge λ_c, we have computed the inverse participation ratio (IPR) for each eigenmode (characterized by eigenvalue λ and wave function $|\psi\rangle$)

$$\nu^{-1} = \int d^4x \, \langle \psi(x)|\psi(x)\rangle^2. \tag{2.1}$$

If an eigenmode is uniformly extended over the whole volume, $\langle\psi(x)|\psi(x)\rangle = \frac{1}{V}$, $\forall x$ the participation ratio becomes $\nu = V$, while for a maximally localized mode at x_0 with a scalar density $a^4\langle\psi(x)|\psi(x)\rangle = \delta_{x,x_0}$ one gets $\nu = a^4$. We can then define a relative eigenmode volume $r(\lambda) = \frac{\nu(\lambda)}{V}$. On the left side of Fig. 2 we present $\langle r(\lambda)\rangle$, averaged over small bins with bin size $\Delta\lambda = 0.005/a$.

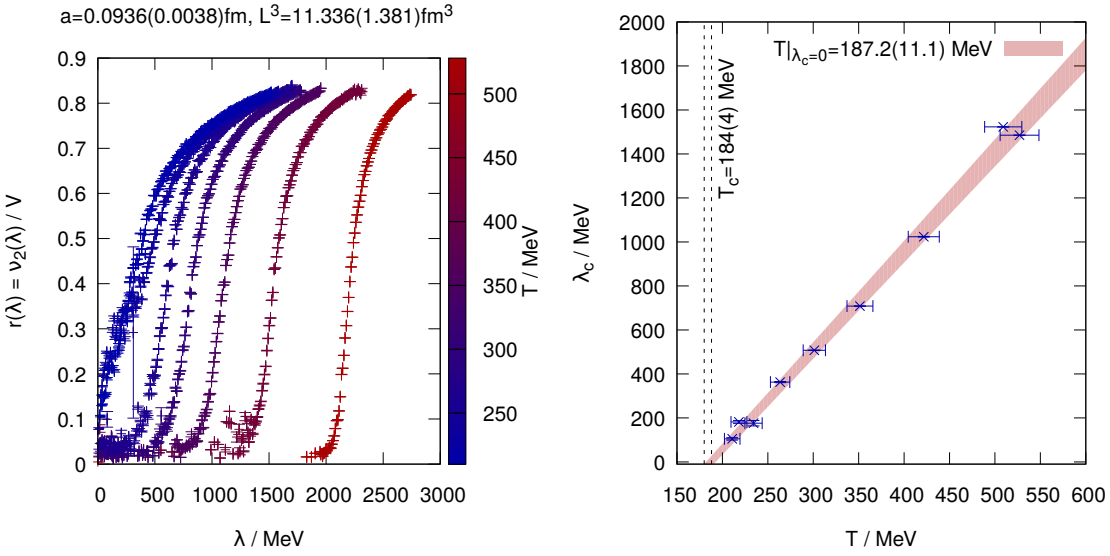

Figure 2: *Left*: The relative eigenvector volume inside bins of width $\Delta\lambda = 0.005/a$ for several temperature ensembles of the A370 configurations. *Right*: The mobility edge $\lambda_c(T)$ is linear in the temperature. The temperature of the chiral transition was taken from [20].

From a fit to $\langle r(\lambda)\rangle$ we determined the inflection point of the curve and used this as an estimate for λ_c. This coincides with the point where fluctuations within each bin are maximal. Other criteria applied to the relative eigenmode volume have yielded qualitatively the same results.

The estimates for λ_c from the A370 and the D370 meta-ensembles imply, that the mobility edge vanishes at the temperature of the chiral crossover, that was determined in [20]. It also agrees well with a linear function of the temperature, which can be seen on the right side of Fig. 2. In particular there is no evidence of curvature, as observed with staggered quarks in [16].

3. Localization and Polyakov loop

Localization seems to be caused by some gauge-invariant objects that apparently do not exist below T_c but become influential with increasing temperature. Such objects would represent the analog to the disorder in the condensed-matter Anderson models. A good candidate for such a local quantity is defects in the Polyakov loop

$$l(\vec{x}) = \frac{1}{N_c}\mathrm{tr}\,\mathcal{P}e^{\int_0^\beta dtA_4(\vec{x},t)}, \tag{3.1}$$

the trace of the local holonomy (or its real part Re $l(\vec{x})$).

In [11] and [23] the connection between the local real-valued $l(\vec{x})$ and the eigenmodes of the Dirac operator has been studied for SU(2) gauge theory. It has been found that the localized modes

are trapped in sinks of $l(\vec{x})$. In [24] an Anderson-like Ising model has been designed to mimick the effect of the Polyakov loop able to cause localization. In [17] this correlation has been studied in full QCD with $N_f = 2$ Möbius Domain-Wall fermions.

To draw the connection of the modes (which are defined with respect to the original gauge field configurations) with the Polyakov loop of the latter requires some amount of gauge field smearing. To remove UV-fluctuations, the gauge configurations were smoothed with the help of Gradient flow (with respect to the Iwasaki gauge action that was used here, until a flow time $a^2\tau = 4.0$).

We observe that the regions, where Re $l(x)$ is small, form clusters of small size and are spatially localized at the same positions where the chiral zero modes in the corresponding configuration are localized.

We have studied for three classes of modes the correlation between the scalar eigenmode density $p(x) = \langle \psi(x) | \psi(x) \rangle$ and the local Polyakov loop, which is shown in Fig. 3 for $T = 351$ MeV. The horizontal line indicates the density $p(x) = \frac{1}{V}$. If a mode is homogenously extended throughout the whole volume, its density would collapse on this line. We observe, that both the zero modes and the localized non-zero modes are strongly anticorrelated with the real part of the Polyakov loop (left and middle panel of figure 3). In regions, where Re $l(x)$ is large, these modes are strongly supressed. Delocalized modes, in contrast, appear to be mostly indifferent with respect to the Polyakov loop, and are spread in a small stripe around the $\frac{1}{V}$-line (right panel). Indeed, negative real part values of the Polyakov loop appear to be acting as source for localization, in analogy to the random on-site potential in the condensed matter Anderson model. This conjecture agrees very well with earlier findings [17] based on Domain-Wall quarks.

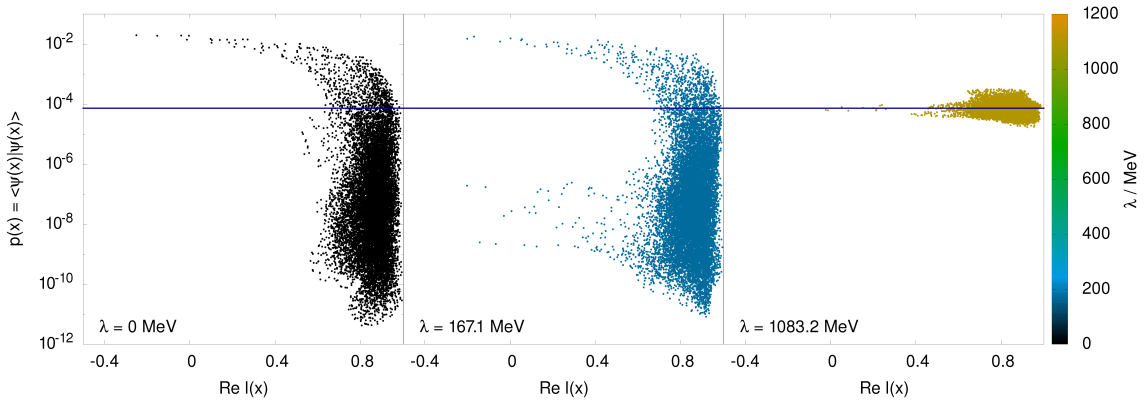

Figure 3: Three typical eigenmodes correlated with the local Polyakov loop at $T = 351$ MeV $\approx 1.91T_c$. *Left*: A chiral zeromode ($\lambda = 0$ MeV). *Middle*: A localized nonzero mode ($\lambda = 167.1$ MeV $\approx 0.24\lambda_c$). *Right*: An extended nonzero mode ($\lambda = 1083.2$ MeV $\approx 1.53\lambda_c$).

In the complex Polyakov plane, the eigenmodes localize in regions, that are close to the boundary of the $l(x)$ scatter plot and the nontrivial centre elements of SU(3), which is shown in the left and middle panel of Fig. 4 for the temperature $T = 218$ MeV $\approx 1.18T_c$. Localization is reflected in a concentration close to regions of the plot, where two or three eigenvalues of the local holonomy are close to being degenerate. In the right panel of Fig. 4, however, we see a delocalized mode being uncorrelated to $l(x)$.

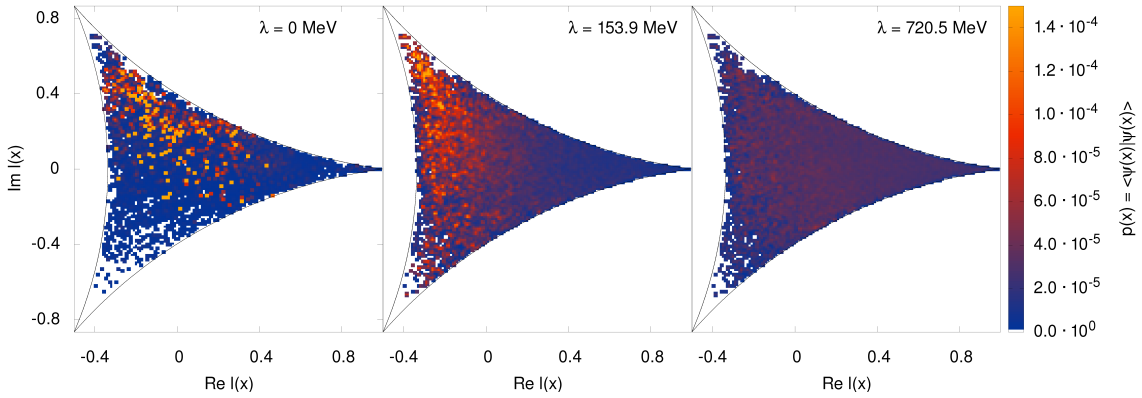

Figure 4: Three typical eigenmodes located in the complex Polyakov loop plane at $T = 218$ MeV $\approx 1.18T_c$. *Left*: A chiral zeromode ($\lambda = 0$ MeV). *Middle*: A localized nonzero mode ($\lambda = 153.9$ MeV $\approx 0.85\lambda_c$). *Right*: An extended nonzero mode ($\lambda = 720.5$ MeV $\approx 3.97\lambda_c$).

4. Conclusion and outlook

We have presented studies of the Anderson transition going on within the Dirac operator spectrum for overlap fermions on the background of gauge configurations from $N_f = 2+1+1$ flavour QCD. It was found, that the temperature dependence of the moblility edge agrees well with a linear extrapolation, and the localized regime disappears at the chiral crossover temperature. We confirmed the conjecture, that negative valued local Polyakov loop acts analogously to the impurities in the condensed matter Anderson model, causing localization.

In order to shed more light on the connection between mode localization and the topological structure of QCD, we have also studied the local gluonic topological charge density and its effect on Dirac eigenmode localization. In [22] it has been found that local topological objects, as described by the dilute instanton gas model, cannot entirely explain eigenmode localization.

It is, however, remarkable, that the overlap

$$O_5(\lambda) = \frac{\int d^4x q(x) p_5(x)}{\frac{1}{2}\int d^4x \left((q(x))^2 + (p_5(x))^2\right)} \tag{4.1}$$

between the topological density $q(x) = \frac{g^2}{16\pi}\varepsilon_{\mu\nu\rho\sigma}F^a_{\mu\nu}(x)F^a_{\rho\sigma}(x)$ and the pseudoscalar density $p_5(x) = \langle\psi(x)|\gamma_5|\psi(x)\rangle$ of individual modes differs drastically between the localized and the extended spectral regions, see Fig. 5. The difference increases with temperature. This effect will be subject to further investigations.

References

[1] P. W. Anderson. *Phys. Rev.*, 109:1492–1505, 1958.

[2] M. A. Halasz and J. J. M. Verbaarschot. *Phys. Rev. Lett.*, 74:3920–3923, May 1995.

[3] Tamas G. Kovacs. *Phys. Rev. Lett.*, 104:031601, 2010.

[4] Tamas G. Kovacs and F. Pittler. *Phys. Rev. Lett.*, 105:192001, 2010.

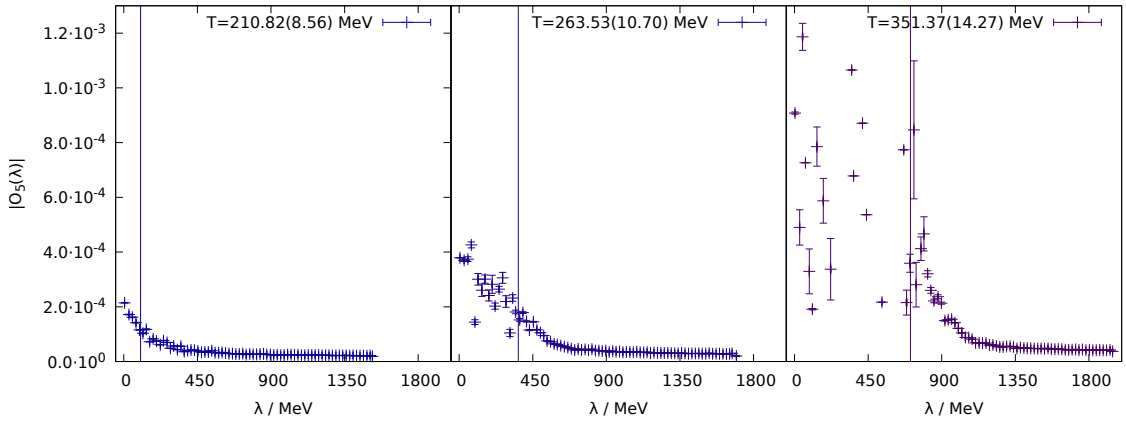

Figure 5: The overlap of the gluonic topological density and the pseudoscalar density. The mobility edge is indicated with a vertical line.

[5] F. Bruckmann, S. Keppeler, M. Panero, and T. Wettig. *Phys. Rev.*, D78:034503, 2008.

[6] B. Klein and J. J. M. Verbaarschot. *Nucl. Phys.*, B588:483–507, 2000.

[7] J. J. M. Verbaarschot and T. Wettig. *Ann. Rev. Nucl. Part. Sci.*, 50:343–410, 2000.

[8] A. M. Halasz and J. J. M. Verbaarschot. *Phys. Rev. Lett.*, 74:3920–3923, 1995.

[9] P. H. Damgaard, Urs M. Heller, R. Niclasen, and K. Rummukainen. *Nucl. Phys.*, B583:347–367, 2000.

[10] R. V. Gavai, S. Gupta, and R. Lacaze. *Phys. Rev.*, D77:114506, 2008.

[11] T. G. Kovacs, F. Pittler, F. Bruckmann, and S. Schierenberg. *PoS*, LATTICE2011:200, 2011.

[12] S. M. Nishigaki, M. Giordano, T. G. Kovacs, and F. Pittler. *PoS*, LATTICE2013:018, 2014.

[13] L. Ujfalusi, M. Giordano, F. Pittler, T. G. Kovacs, and I. Varga. *Phys. Rev.*, D92(9):094513, 2015.

[14] L. Ujfalusi and I. Varga. *Phys. Rev. B*, 91(18), 2015.

[15] M. Giordano, S. D. Katz, T. G. Kovacs, and F. Pittler. *PoS*, LATTICE2014:214, 2014.

[16] M. Giordano, T. Kovacs, F. Pittler, L. Ujfalusi, and I. Varga. *PoS*, LATTICE2014:212, 2014.

[17] G. Cossu and S. Hashimoto. *JHEP*, 06:056, 2016.

[18] H. Neuberger. *Phys. Lett.*, B417:141–144, 1998.

[19] F. Burger, G. Hotzel, M. Müller-Preussker, E.-M. Ilgenfritz, and M. P. Lombardo. *PoS*, Lattice2013:153, 2013.

[20] F. Burger, E.-M. Ilgenfritz, M. P. Lombardo, M. Müller-Preussker, and A. Trunin. *J. Phys. Conf. Ser.*, 668(1):012092, 2016.

[21] F. Burger, E.-M. Ilgenfritz, M. P. Lombardo, M. Müller-Preussker, and A. Trunin. *Nucl. Phys.*, A967:880–883, 2017.

[22] T. G. Kovacs and R. A. Vig. *Phys. Rev.*, D97(1):014502, 2018.

[23] F. Bruckmann, T. G. Kovacs, and S. Schierenberg. *Phys. Rev.*, D84:034505, 2011.

[24] M. Giordano, T. G. Kovacs, and F. Pittler. *JHEP*, 04:112, 2015.